J Arid Land (2023) 15(7): 827–841
https://doi.org/10.1007/s40333-023-0021-8

Science Press   Springer-Verlag

Morphological change and migration of revegetated dunes in the Ketu Sandy Land of the Qinghai Lake, China

WU Wangyang[1,2], ZHANG Dengshan[2], TIAN Lihui[2*], SHEN Tingting[1], GAO Bin[1], YANG Dehui[1]

[1] School of Earth Sciences, East China University of Technology, Nanchang 330013, China;
[2] State Key Laboratory of Plateau Ecology and Agriculture, Qinghai University, Xining 810016, China

Abstract: Alpine revegetated dunes have been barely researched in terms of morphological change and migration within its regional aeolian environments. To reveal the sand-fixing and land-reforming mechanisms of artificial vegetation, we observed the morphology and migration of four dunes with four revegetated types (*Hippophae rhamnoides* Linn., *Salix cheilophila* Schneid., *Populus simonii* Carr., and *Artemisia desertorum* Spreng.) using unpiloted aerial vehicle images and GPS (global positioning system) mapping in 2009 and 2018. Spatial analysis of GIS (geographic information system) revealed that the revegetated dunes exhibited a steady progression from barchan dune shapes to dome or ribbons shapes mainly through knap planation, wing amplification, and slope symmetrization. Generally, conditions of northern aspects, smaller slope degree, and larger altitude of unvegetated dunes would suffer more serious wind erosion. The southward movement of dune wings with a migration speed of 2.0–5.0 m/a and the alternating motion of sand ridges in eastwestern directions led greater stability in revegetated dunes. The moving distances of revegetated dunes remarkably changed in patterns of quadratic or linear function with depositional depth. Compared with unvegetated dunes, the near-surface wind velocity of revegetated dunes decreased by 20%–30%, which led to heavy accumulation in low-flat dunes and erosion in high-steep dunes, but all vegetation species produced obvious sand-fixing benefits (100%–450% and 3%–140% in the lower and higher dune scales of revegetated dunes, respectively) with decreasing sand transport rates and increasing coverages. In practice, the four vegetation species effectively anchored mobile dunes by adapting to regional aeolian environment. However, future revegetation efforts should consider optimizing dune morphology by utilizing *H. rhamnoides* as a pioneer plant, *S. cheilophila* and *P. microphylla* in windward and northward dune positions, and *A. desertorum* in a sand accumulative southward position. Also, we should adjust afforestation structure and replant some shrub or herbs in the higher revegetated dunes to prevent fixed dune activation and southward expansion.

Keywords: artificial vegetation; dune morphology; migration; aeolian factor; species difference

Citation: WU Wangyang, ZHANG Dengshan, TIAN Lihui, SHEN Tingting, GAO Bin, YANG Dehui. 2023. Morphological change and migration of revegetated dunes in the Ketu Sandy Land of the Qinghai Lake, China. Journal of Arid Land, 15(7): 827–841. https://doi.org/10.1007/s40333-023-0021-8

1 Introduction

Revegetated dune is one of manually inverted dune types, which is ecologically restored with artificial vegetation. This pattern dune appears to represent heavy aeolian activity that needs

*Corresponding author: TIAN Lihui (E-mail: lhtian@qhu.edu.cn)
Received 2023-01-31; revised 2023-05-12; accepted 2023-05-17

urgent control of sand fixation (Wang, 2000; Wang and Zhao, 2005). Revegetation changes dune morphology by influencing surface airflow, wind erosion, and sediment transport (Leenders et al., 2011; Follett and Nepf, 2012; Hesp et al., 2019). Revegetated dunes become fixed or semi-fixed dunes due to the vegetative growth, leading to obvious differences in dune morphology and migration before and after revegetation (Durán and Herrmann, 2006; Barchyn and Hugenholtz, 2012). Then, the dunes gradually develop into longitudinal or dome dunes owing to weakening aeolian activity (Zhu, 1963; Qian et al., 2019). The long-term ecological restoration effects of revegetation are uncertain, yet they may be predicted from observations of dune morphology and aeolian characteristics (Miyasaka et al., 2014).

Previous research has primarily examined the geometric characteristics and morphodynamic process of dunes in their bare state, without the implementation of any control measures (Anthonsen et al., 1996; Liu et al., 2018; Bhadra et al., 2019; Xiao et al., 2021). In China, the morphological evolution of sand dunes, including barchan, linear, and dome dunes, has been comparatively studied. Dome-shaped dunes may evolve into barchan dunes, and the latter can develop into linear dunes under the influence of wind regime, drift potential, sand supply, and migration rate (Momiji et al., 2002; Rozier et al., 2019). Additionally, natural sandy vegetation may play an important role in the formation of nebkhas, and linear and parabolic dunes (Hasi et al., 2013; Samuel et al., 2022). Artificial vegetation community conserves soil and water by restraining sand blowing and wind erosion (Xu et al., 2015). Microtopography and microclimate lead to aeolian differences in different parts of revegetated dunes, like strong wind erosion always occurs in upwind part and dune knap, and heavy sand accumulation appears in downwind part and bilateral slope toes (Gillies et al., 2014; Walker et al., 2022). Therefore, studies of revegetated dune morphology and aeolian feature changes should focus on vegetation-air-soil interactions (Pike et al., 2009; Li et al., 2021; Yamasaki et al., 2021).

Remote sensing image sources such as Landsat, Google Earth, SPOT (small programmable object technology), and QuickBird are widely used for large- and medium-scale dune identification and quantification (Bubenzer and Bolten, 2008; Hugenholtz et al., 2012). Some traditional methods of field observation and gauging like DGPS (differential GPS), 3D laser scanning UAV (unmanned aerial vehicle), and fingerprint are employed for vegetated dune morphology observation and 3D modeling (Louis, 2019; Rominger and Meyer, 2019; Zheng et al., 2022). Advanced field gauging devices can improve the resolution of small-scale dune morphology and migration observation in revegetated areas (Telbisz and Orsolya, 2018).

Sandy land in China is subject to a high frequency and velocity of sand moving wind, which causes strong wind erosion and sand burial in alpine barchan and dome dunes (Zhang et al., 2018; Pang et al., 2020; Hu et al., 2021; Cao et al., 2022). But there is a lack of morphological and aerodynamic analysis of revegetated dunes formation and evolution, associated with aeolian factors (Li et al., 2017; Chang et al., 2021). Therefore, we examined the morphology and migration characteristics of revegetated alpine dunes through detailed analysis of dune scales and positions and vegetation species differences with the aim of identifying the relationships of regional microtopography and aerodynamics with vegetation, and making further predictions of revegetated dune evolution and stabilization.

2 Materials and methods

2.1 Study area

The Ketu Sandy Land located in eastern Qinghai Lake, northwestern China (Fig. 1a). The local climate integrated with the East Asian monsoon, northwestern arid and alpine climate of China. Data from the regional meteorological station indicate a cold, windy, and semi-arid climate, the annual mean temperature and precipitation are 0.7℃ and 370.0 mm, respectively, and the prevailing northerly wind has a velocity of over 4.5 m/s and a frequency of nearly 35%. A strong wind-sand activity in this sandy land is reflected by a high sand drift potential of nearly 300 VU/a

dominated in the west and northwest wind directions (Zhang et al., 2016). Large areas of the Ketu Sandy Land belong to severe and extremely severe desertification lands, and mainly consists of short barchan dunes, mega-dunes, and transversal sand ridges. Since the early 1980s, the local government has taken lots of measures, including enclosure, mechanical barriers, and vegetation afforestation, to control desertification and accelerate ecology restoration. Since 2008, over 20 artificial vegetation species have been transplanted to different types of sand dunes. Most of revegetated dunes had developed to vegetation communities after 3–5 a, and became a vegetative experimental demonstration area (VEDA) of alpine desert control (Wu et al., 2019).

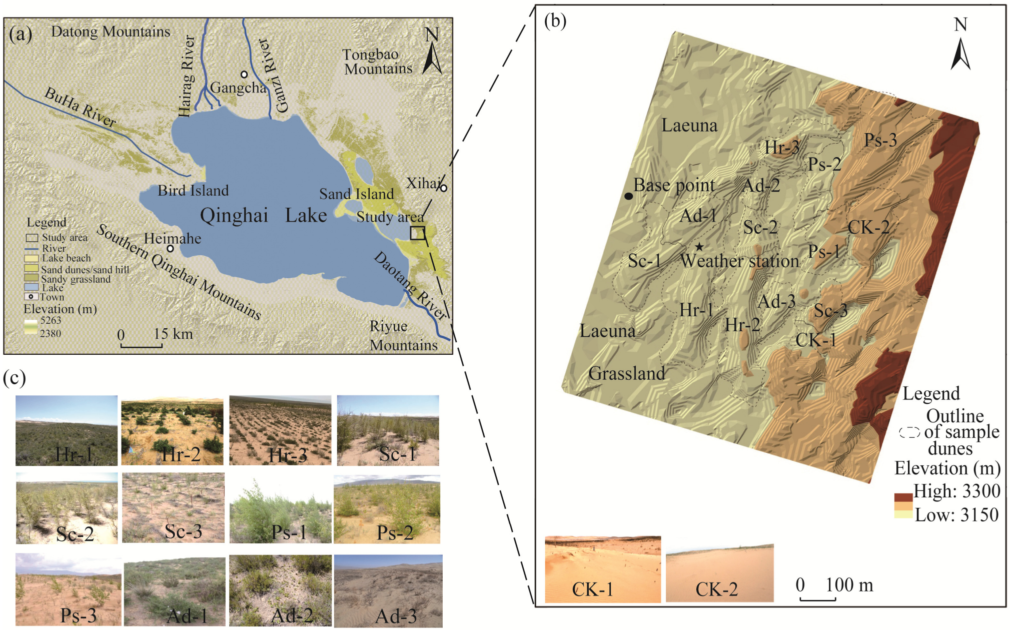

Fig. 1 Location of study area (a) and design of sample dunes (b and c) in the Ketu Sandy Land of the Qinghai Lake, China. Hr-1, Hr-2, and Hr-3, *H. rhamnoides* dunes; Sc-1, Sc-2, and Sc-3, *S. cheilophila* dunes; Ps-1, Ps-2, and Ps-3, *P. sylvestris* dunes; Ad-1, Ad-2, and Ad-3, *A. desertorum* dunes; CK-1 and CK-2, reference sand dunes. The abbreviations are the same in the following tables and figures.

2.2 Sample design

In the September of 2008, four revegetated dunes types (*H. rhamnoides*, *S. cheilophila*, *P. sylvestris*, and *A. desertorum*) in the VEDA were selected as sample dunes (Fig. 1b and c). They were almost purely bare shifting dunes similarly in regional aeolian climate and soil properties before plantation. Two or three topographic scales (low-flat scale, medium scale, and high-steep scale) differed from primary dunes absolute height, relative height, and slope gradient were arranged for each revegetated dune type (Table 1). Additionally, two shifting bare dunes (CK-1 and CK-2) were set as reference sand dunes. All sample dunes were originally barchan formations stretching from northeast to southwest, and the windward slope faced northern and northwestern directions.

2.3 Data sources and analysis

2.3.1 Dune morphology and migration

In the October of 2009 and 2018, the high-resolution images of the VEDA were obtained by the UAV (Dajiang Spirit 4, Shenzhen Dajiang Innovation Technology Co. Ltd., Shenzhen, China), which equipped with camera lens of 4 mm focal length. We controlled a flying height of 120 m and a tracing velocity of 3 m/s. The camera of the UAV took photos vertically with a shooting interval of 3 s, and their course overlap and lateral overlap were ensured both higher than 70%. During the periods, we used GPSmap 60CSx global positioning system receiver (Garmin, 2D

Table 1 Basic condition of each sample dune investigated in 2009

Sample dune	Altitude (m)	Dune height (m)	Dune shape	Sample area (hm^2)	Slope degree (°)	Dune scale	Soil density (g/cm^3)	Vegetation density (individuals/hm^2)
Hr-1	3186.17	8.17	Barchan	2.89	<5	Low-flat	1.57	4500
Hr-2	3188.13	10.13	Barchan chain	2.64	5–10	Medium	1.69	4500
Hr-3	3190.11	13.00	Barchan chain	1.29	10–15	High-steep	1.58	4500
Sc-1	3183.38	5.38	Barchan	1.66	5–15	Low-flat	1.52	4500
Sc-2	3186.31	8.31	Barchan	0.77	10–15	Medium	1.62	2500
Sc-3	3189.89	11.89	Barchan	0.66	>25	High-steep	1.63	3250
Ps-1	3189.15	11.15	Beam dune	1.14	5–10	Medium	1.57	2500
Ps-2	3189.21	11.21	Barchan	1.07	10–15	Medium	1.59	2500
Ps-3	3195.64	17.64	Barchan chain	2.15	>25	High-steep	1.74	2500
Ad-1	3184.90	7.80	Barchan	1.07	<5	Low-flat	1.51	50,000
Ad-2	3185.92	7.92	Barchan chain	0.49	5–15	Low-flat	1.60	2500
Ad-3	3188.31	10.31	Barchan	0.63	>25	Medium	1.61	4500
CK-1	3189.90	11.90	Barchan	0.37	<5	Medium	1.55	0
CK-2	3192.28	14.28	Barchan chain	1.48	5–10	High-steep	1.55	0

positioning accuracy of 1.0 m) to track the dunes outer edges, slopes, and sand ridges with an average interval of 5 m (Zhang et al., 2018). All the GPS sampling data were used to match and correct with the UAV image points. Importing the UAV images to the software of PhotoScan, and making a series of picture processing of target point alignment, mesh generation, and texture recognition, we got digital orthoimage (DOM) and 3D terrain data of all sample dunes. Then, the DOM and GPS sampling points were managed with the software of ArcGIS v.10.2 to extract various dune morphology parameters like the area of sand dunes (A, m^2), the length of dune ridges (L_0, m), bilateral slopes degrees (S_1, westerly slope degree, °; S_2, easterly slope degree, °), and slope lengths (L_1, westerly slope length, m; L_2, easterly slope length, m). When each sample dune's spatial position and outline were extracted and overlaid with 3D terrain elevations (E), the dune's absolute height (H_0) and relative heights (H_1 and H_2) were identified as the following Equation 1. In the differences of two periods' DEM (digital elevation model) data (ΔE), the erosion position (ΔE<0) and sand deposition position (ΔE>0) of sample dunes were clearly presented in the changed elevation grid net under the spatial analyze function of ArcToolbox.

$$H_0 = E_0 - E_B;\ H_1 = E_0 - E_1;\ H_2 = E_0 - E_2, \tag{1}$$

where H_0 (m), H_1 (m), and H_2 (m) are the elevation differences of the highest point of dunes knap (E_0, height above sea level) with the base point (E_B, besides in the road approaching to the lake level altitude), the lowest point of the westerly slope toe (E_1), and the easterly slope toe (E_2), respectively.

Dune volume (V, m^3) was calculated by the surface function of 3D Analyst Tools of ArcGIS v.10.2. Making a volume subtraction between two periods (ΔV), the sand expansion area (ΔV>0) and direction, we determined sand deposition amount (W) and intensity (W_i) by Equations 2 and 3. Migration of different positions of dune was decided by two periods' spatial location of outline edges and sand ridges, the annual migration speed (M, m/a) was averaged by 5–10 space distance lines under spatial distance analysis of ArcGIS v.10.2.

$$W = \Delta V \times \rho, \tag{2}$$

$$W_i = \frac{W}{A \times n}, \tag{3}$$

where ρ, A, and n are the dunes' soil density (kg/m^3), the vertical projected area (m^2), and the

count of years, respectively. If W and W_i are larger than 0, it indicates the dune's sand deposition phenomenon, conversely, it produces wind erosion and sand transport.

2.3.2 Wind velocity and direction

In the December or March of 2009 and 2018, five sets of portable anemometers (the self-counting wind speed interval was 30 s, and the errors of velocity and direction are less 0.5 m/s and 5°, respectively) were applied to collect surface wind velocity and direction, one set was installed in a fixed height of 1.0 m to be a base station for the mobile points calibration under the same time (Eq. 4), and the other four sets were installed on a homemade bracket (steel material, 2.5 m high) as a mobile device, and placed on four side bars of the bracket in the heights of 0.5, 1.0, 1.5, and 2.0 m, respectively. Fixed device stood in the base point, and the mobile device worked in each sample dune parts including knap, the easterly and westerly toe-slope and mid-slope, and the north and south wings. Wind data of over 6.0 m/s averaged in continuous 10 min would be screened out for some comparisons of dunes position, vegetation species, and yearly change. Threshold wind velocity of sand-driving (V_t) of all sample dunes and the surface roughness (z_0, Eq. 5) were observed and calculated from field wind profiles.

$$V'(z)=\frac{V_m(t_0,z=1)}{V_m(t,z=1)}\times V(t,z=1), \tag{4}$$

where $V'(z)$ is the standardized wind velocity (m/s) at height z (m); and V_m (t_0, z=1), V_m (t, z=1) are the measured wind velocity of base point at 1 m height at time t_0 and t, respectively (m/s); and $V(t, z=1)$ is the wind velocity of re-vegetated dune points at 1 m height (m/s).

$$\lg z_0=\frac{\lg z_2-\lg z_1}{1-A};\ A=V_{2.0\mathrm{m}}-V_{0.2\mathrm{m}}\ , \tag{5}$$

where $V_{2.0\mathrm{m}}$ and $V_{0.2\mathrm{m}}$ are the wind velocities in heights of z_1 and z_2, respectively (m/s).

2.3.3 Sediment transport and deposition

From 2009 to 2018, sand transport amount was measured by a vertical sand sampler with 30 catchers (2 cm high×5 cm wide) placed at different dunes positions. Every time, sand samples collected sands from wind-sand flow for 10 min, and repeated the work at least three times. Then, sand samples were fetched back with valve bags from the sand catchers and weighted using a 1/1000 balance scale. Sand transport rate (TR, g/(cm^2·min)) was transferred from the total sand amount of 30 catchers by Equation 6.

$$\mathrm{TR}=\frac{\sum T_i}{s\times t}, \tag{6}$$

where T_i is the sand amount of i layer fetcher (i=1, 2, 3, ⋯, 30); s is the vertical sectional area of the sand sampler (s=300 cm^2), and t is the time of collecting sand (t=10 min).

In January of 2010, 3–5 polyvinchlorid (PVC) tubes (40 cm long and 3 cm in diameter) were inserted surface soil with 25 cm buried and 15 cm exposure in westerly slope, top, and easterly slope of sample dunes. We measured the exposure length (l) of tubes every month, and tested the exposure length change (Δl) in the past 10 a for judging wind erosion ($\Delta l<0$) or sand deposition ($\Delta l>0$). Beside PVC pipe, five 250 cm^3 plastic bottles were buried at the top of each plot for evaluating erosion (collecting sand) or deposition amount (weighting every month). Based on seasonal aeolian activity difference, we calculated the yearly deposition intensity W_i (t/(hm^2·a)) given by Equation 7.

$$W_i=\frac{\sum m_i}{s}\times 100, \tag{7}$$

where m_i is the bottle sand amount in i (i=1, 2, 3, ⋯, 12) month (g); and s is the sand entrance area of each bottleneck (28.3 cm^2).

To analyze the difference significance and relationships among morphology, migration, and aeolian activity, we used the Origin v.18.0 software to make significance test (t-test and P-value)

and curve fitting (R^2, fitting coefficient). Correlations of bivariate analysis (correlation coefficient, r) and one-way ANOVA (analysis of variance) were used to explain parameter differences.

3 Results

3.1 Dune morphology

3.1.1 Shape, area, and volume

Most of barchan dunes developed into dome or ribbon dunes, two dimensional area (A) and volume (V) changes of revegetated dunes were more stable than those of reference dunes. Sand dune area variation (ΔA) in 2009 and 2018 showed a slight increase (ΔA<0.2 hm^2) in most dunes in addition to low-flat scales of *S. cheilophila* dunes and *A. desertorum* dunes (Fig. 2). With positive correlation to 2D-area (r>0.88), the volume of sand dunes mainly showed increases of 0.01×10^6–0.20×10^6 m^3, except in some high-steep scales of *H. rhamnoides*, *S. cheilophila*, and reference sand dunes. In general, most low- and medium-scale dunes expanded horizontally, showing obvious sand accumulation functions.

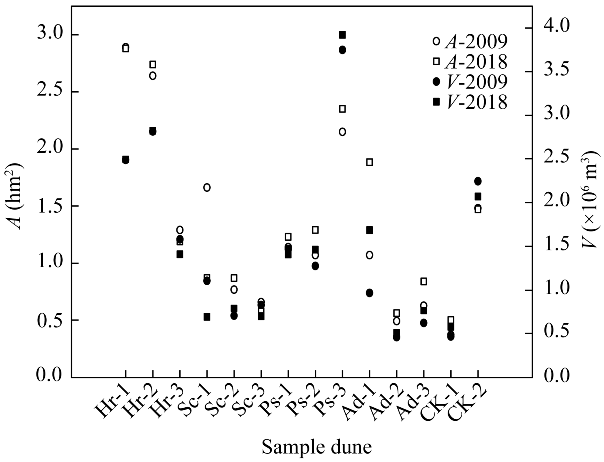

Fig. 2 Area (A) and volume (V) of the sample dunes in 2009 and 2018

3.1.2 Height and slope

Artificial vegetation affected the outline edge position and shape of the dunes. In the past decade, H_0 (absolute height) values of *H. rhamnoides* and *S. cheilophila* dunes changed less than those of other sample dunes (1.8 m<H_0<0.5 m) (Figs. 3 and 4a). H_0 of higher dunes consistently experienced greater reductions than those of lower and medium dunes (0.010<P<0.014). Additionally, variations in H_1 (relative height; 0.5 m<ΔH_1<1.2 m) were larger than those in H_2 (relative height; –1.5 m<ΔH_2<0.0 m) for the majority of sample dunes. In comparison, *S. cheilophila* and *P. simonii* dunes with higher scales suffered more serious wind erosion on their westward slopes, and *H. rhamnoides* and *A. desertorum* dunes with all scales experienced clearly sand deposition on their eastward slopes.

Wind blowing and sand burial caused surficial undulation in different parts of sand dunes, mainly affecting slope degree (S) and aspect (D) (Fig. 4b and c). The slope degree of almost all lower and medium dunes' knap exhibited little variation (–2°<ΔS<2°) except that of higher *H. rhamnoides* and *S. cheilophila* dunes (8°<ΔS<12°). The bilateral slope positions changed heavier in slope degree from 5°–10° to 7°–20° in the past decade. There were large vegetation and dune position differences in slope degrees (P<0.050) for most sample dunes, the great slope degree changes mainly occurred in west slope positions and species of *S. cheilophila* and *P. simonii* dunes (3°<ΔS<9°).

Changes in sand dune aspect corresponded to changes in surface height and slope degree (Fig.

4c). As all sample dunes fully stretched from northeast to southwest and fell slowly from north to south, the top position of dunes presented aspects of southwest-south-southeast, and changed by less than 23°. The slope aspects shifted from west-southwest and east-northeast to northwest and southeast (ΔD<45°), respectively, with the most significant changes occurring in high-steep *H. rhamnoides* and low-flat *S. cheilophila* dunes.

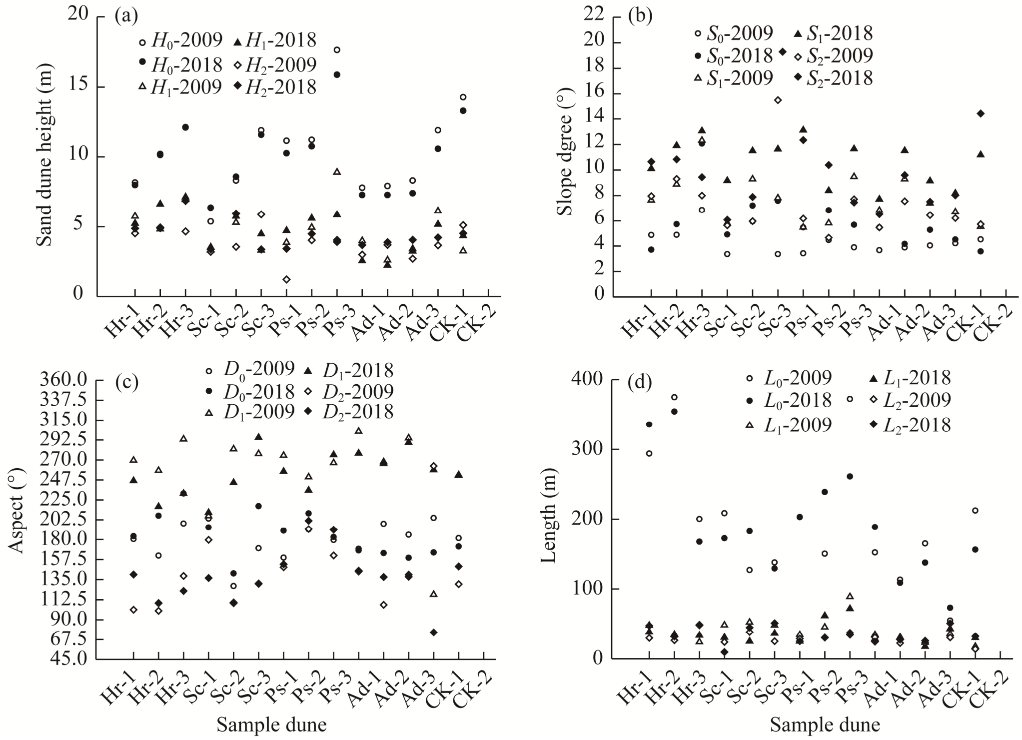

Fig. 3 Dune morphology parameters of height (a), slope degree (b), aspect (c), and length (d) in 2009 and 2018. H_0, S_0, D_0, and L_0 are the values of dunes ridge of absolute height, slope degree, aspect, and length, respectively; H_1, S_1, D_1, and L_1 are the values of westerly slope of relative height, slope degree, aspect, and length, respectively; H_2, S_2, D_2, and L_2 are the values of westerly slope of relative height, slope degree, aspect, and length, respectively.

3.1.3 Dune slope and ridge length

Prior to revegetation, all the sample dunes faced a heavier sand hazard with a symbol of sand ridge movement. Gradually, sharp ridge changed flat and intermittent with the increased sand-fixing function of artificial vegetation (Fig. 4d). After 10 a, most of low-flat and medium sand dune ridge lengths increased by 20–90 m, especially those of *S. cheilophila* and *P. simonii* dunes (ΔL_0>55 m). In contrast, high-steep sand dunes' ridges narrowed by 10–110 m typically for *P. simonii* and reference dunes. Bilateral slope length corresponded to ridge change and reflected dome shape growth. There was a decrease (ΔL_1< –10 m) in west slope length and an increase (10 m<ΔL_2<25 m) in east slope length of high-steep sand dunes. A continuous decrease in slope-length difference (P<0.050) led to two slope forms becoming symmetrical. Slope morphology of *S. cheilophila* and *P. simonii* dunes changed more significant than those of *H. rhamnoides* and *A. desertorum* dunes.

3.2 Migration

Revegetated sand dunes moved more slowly compared with unrestored shifting dunes. We observed comprehensive differences in dune positions and vegetation species according to outline edge monitoring of moving speed and direction (Fig. 4d). There were three migration patterns: north/northeast-to-south/southwest movement for north and south dune edges, west-to-east movement for westward slope edges, and east-to-west movement for eastward slope edges.

Migration speed (M) varied by vegetation species and dune scales. *S. cheilophila* and *P. simonii* dunes (3.0 m/a$<M<5.0$ m/a) moved southward at a faster speed than *H. rhamnoides* (1.0 m/a$<M<3.2$ m/a) and *A. desertorum* dunes ($M<1.0$ m/a). With the exception of some high-steep scale dunes (2.0 m/a$<M<4.0$ m/a), most of sample dunes slope edges moved eastward or westward slowly ($M<1.5$ m/a).

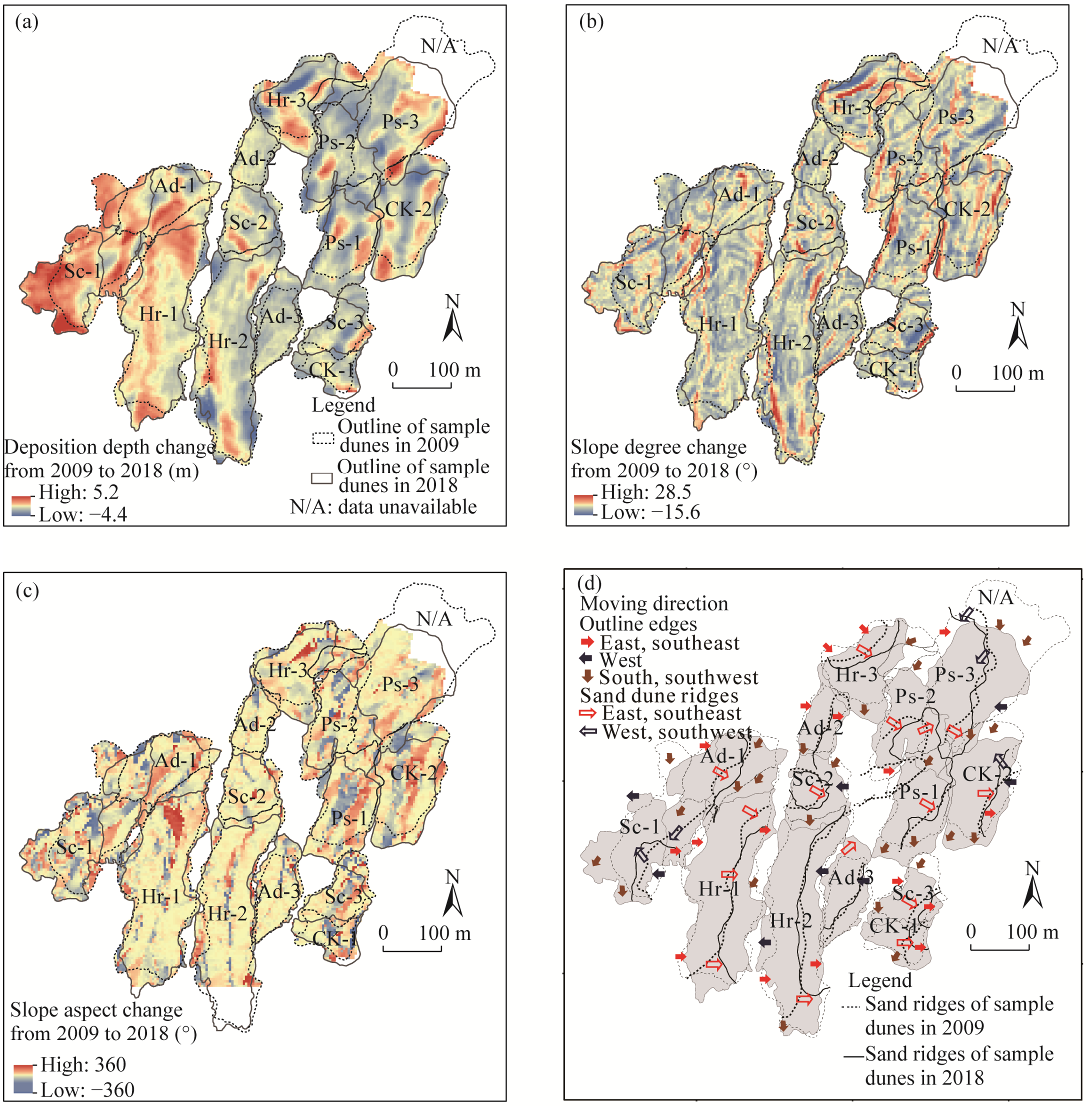

Fig. 4 Changes and spatial distributions of deposition depth (a), slope degree (b), aspect (d), and sand ridge (d) of all sample dunes from 2009 to 2018

Furthermore, most of sample dune ridges moved similarly with outline edges in eastward or southward moving direction, and they changed more prominently in swing part than in the middle part of ridges. The eastward migration phenomenon was mainly observed in *S. cheilophila* and *H. rhamnoides* dunes with the fastest speed of over 2.0 m/a, whereas, a slightly westward movement ($M<0.6$ m/a) in the knap part of ridges mainly happened in high-steep *P. simonii* and *A. desertorum* dunes. Compared with those of reference dunes (1.5 m/a $M_{\text{low-flat}}<3.0$ m/a, 0.5 m/a$<M_{\text{high-steep}}<2.0$ m/a), revegetated dune ridges moved slightly slower for low-flat scales and slightly faster for high-steep scales. Actually, revegetated sand ridges twisted and turned into two swings due to stronger sand-fixing benefits in north and south, with increasing knap deplanation

in the middle. In contrast, reference dune ridges swayed easily with seasons and migration was blocked by adjacent dunes, moving more slightly and slowly than outline edges.

3.3 Wind erosion and sand deposition

We calculated changes of dunes' wind erosive and sand accumulative position, area percentage, and sand deposition rate and intensity based on out edge contours and their elevations of sample revegetated dunes. Different aeolian activities appeared both in dune scales and positions. First, almost all revegetated dunes mainly exhibited sand accumulation in low-flat scale and erosion in medium and high-steep scales (Fig. 5a). The order of deposition intensity among all vegetation species form low to high was the order of reference dunes, *P. simonii*, *S. cheilophila*, *H. rhamnoides*, and *A. desertorum* dunes. Second, knap and north wings were commonly erosive, while south and east slope toes were seriously sand accumulated, especially in low-flat scales of *S. cheilophila*, *H. rhamnoides*, and *A. desertorum* dunes. Third, there were generally larger wind erosion areas (55%–95%) and smaller sand deposition intensities (-33.0×10^3 t/hm^2<W_i< -5.0×10^3 t/hm^2) in higher and steeper scale dunes. In contrast, low-flat scale dunes presented 70%–90% deposition areas and moderate to severe deposition intensities (0.5×10^3 t/hm^2<W_i<110.0×10^3 t/hm^2). Considering the dune scale differences, *A. desertorum* dunes were over-accumulative (W_i>100.0×10^3 t/hm^2), greatly exceeding the deposition intensities of other sample dunes. Fourth, compared with reference dunes, revegetated dunes exhibited heavier sand accumulation and weaker wind erosion. This was evidenced by the low-flat revegetated dunes' distinctive sand-fixing benefits, which changed net sand loss to sand accumulation. Furthermore, medium and high-steep revegetated dunes showed smaller sand-fixing benefits ranging from 3% to 140%, and *P. simonii* and *A. desertorum* exhibited better aeolian control functions than *H. rhamnoides* and *S. cheilophila*.

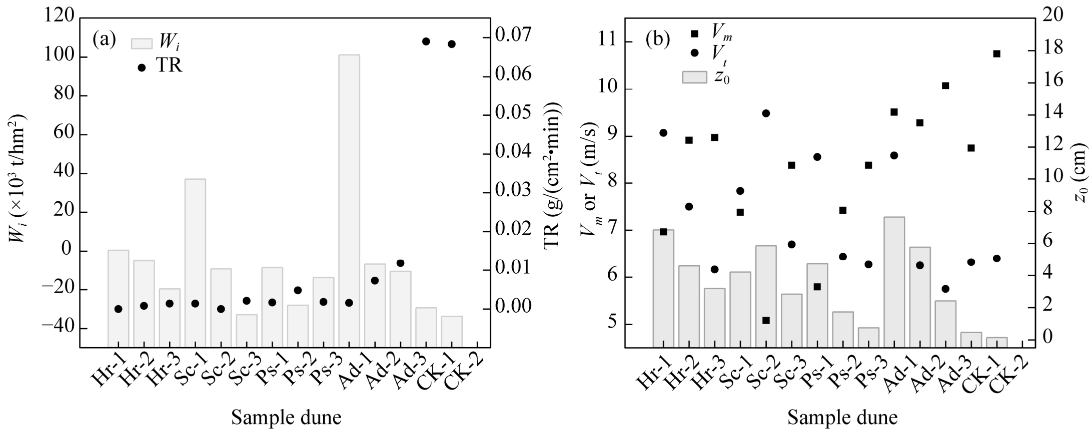

Fig. 5 Aeolian features of sample dunes. (a), W_i (yearly deposition intensity) and TR (sand transport rate); (b), V_m (wind velocity of base point), V_t (wind velocity of sand-driving), and z_0 (surface roughness).

Dune morphology and their aeolian intensity were caused by wind velocity (V_m, 2 m high) and sand transport rate change under an open field wind velocity (V_t, 2 m high) (Fig. 5b). The revegetated dune near-surface wind velocities and sand transport rates decreased by approximately 20%–30% and 70%–100%, respectively. Wind velocity differences among three topographic scales confirmed stronger wind erosion in medium and higher scales, and sand transport rate was always higher in knap position and lower in slopes. Revegetated dunes exhibited slower changes in morphology and migration due to significant increases in threshold wind velocity (1.8 m/s<ΔV_t<3.2 m/s) and surface roughness (2 cm<Δz_0<8 cm). Contrastingly, aeolian environments of low-flat *H. rhamnoides* and *A. desertorum* dunes were weaker than *S. cheilophila* and *P. simonii* dunes, but this inverse relationship was observed in medium and high-steep scales.

3.4 Relationship between morphology and aeolian acitivity

3.4.1 Original topography and deposition depth

Original topography including dunes height, slope degree, aspect, controlled surface airflow direction, and velocity. Based on sand deposition depth distribution in dune configurations of original slope degree–altitude and slope degree–aspect (Fig. 6), we found that deposition depth (ΔE) of different dune positions changed linearly or quadratically with original altitude and slope degree. A negative correlation (r< –0.85) between deposition depth and original altitude existed in majority of revegetated dunes. Deposition depth increased positively with both steepened and flattened slope degree change (ΔS). Slope aspects directly revealed dunes aeolian positions in

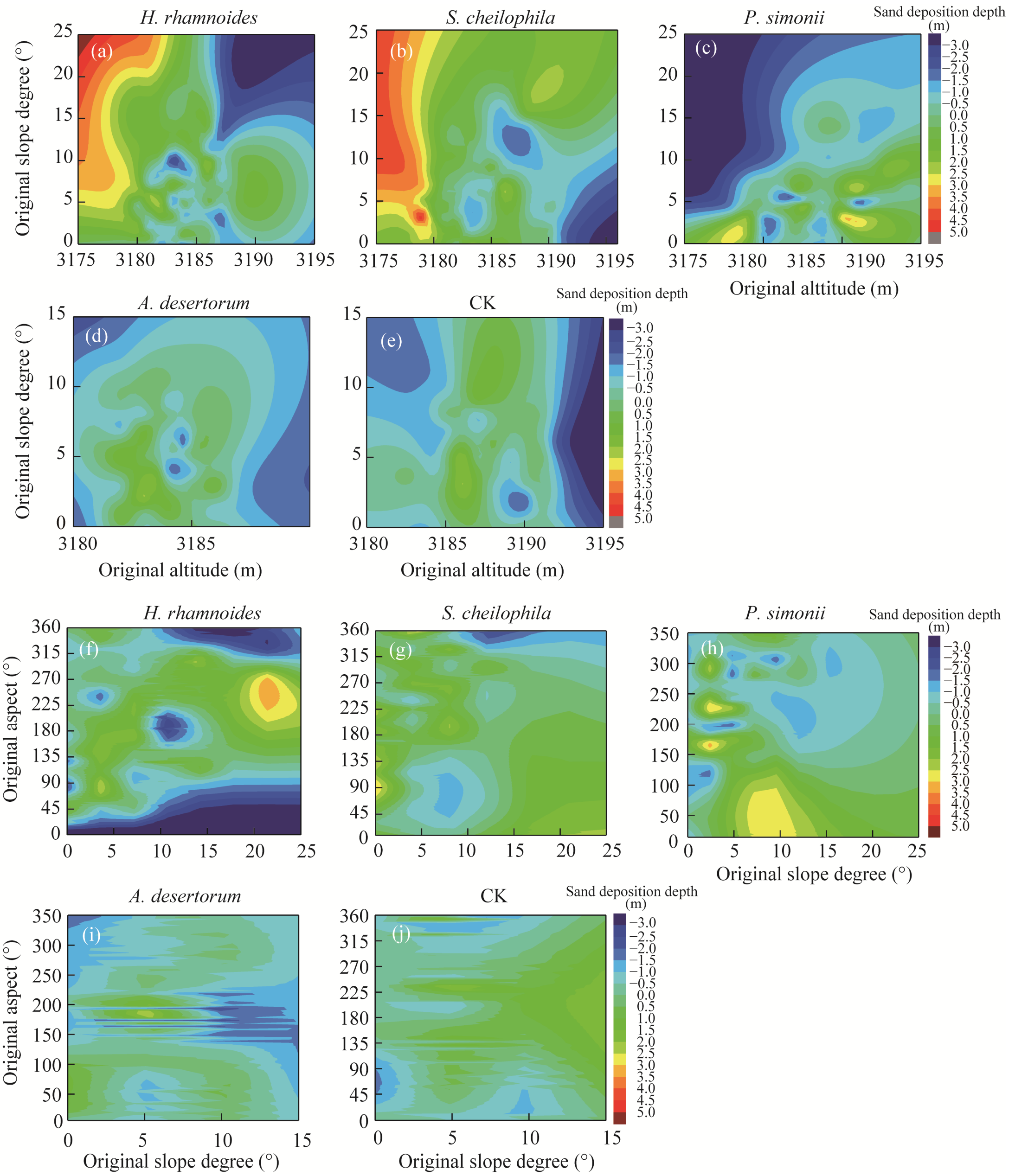

Fig. 6 Relationships of sand deposition depth between original altitude (a–e) and slope degree, and between original aspect and slope degree (f–j) of each sample dune

correspondence with regional leading wind directions, almost all sample dunes showed apparent wind erosion in northwest-north-northeast aspects and sand accumulation in southeast-south-southwest aspects. Additionally, impact of multiple interacting topographic factors was greater than that of single factor. Topographic conditions of northern aspects, smaller original slope degree, and larger original altitude led to more serious wind erosion, whereas dunes with southern aspects, larger original slope degrees, and smaller original altitude were more likely to experience sand accumulation. In terms of vegetation species, *S. cheilophila* and *P. simonii* dunes exhibited strong knap-erosion in northern directions and strong slope toe-deposition in southwestern directions, while *H. rhamnoides* and *A. desertorum* dunes pertained to medium slope-erosion and omni-directional medium deposition.

3.4.2 Migration and deposition depth

Migration distance or speed in different positions of outline edge and sand ridge exhibited remarkable change patterns of quadraticor or linear function with depositional depth (Δl) after significant test (P<0.050) and square test (0.780<R^2<0.950) (Fig. 7; Table 2). Both for southward and westward movement of revegetated dunes, migration distance generally increased with sand deposition depth and erosion depth, suggesting that over wind-erosion and over sand-accumulation led to quick dune movements. Balance values of deposition depth corresponding to the lowest migration distance reflected vegetation ability of anti-erosion or anti-sand burial. All revegetated dunes moved more slowly under balance values of –3.0 to 3.0 cm, comparatively, migrations of *A. desertorum* and *P. simonii* dunes were more sensitive to aeolian activity, compared with *H. rhamnoides* and *S. cheilophila* dunes.

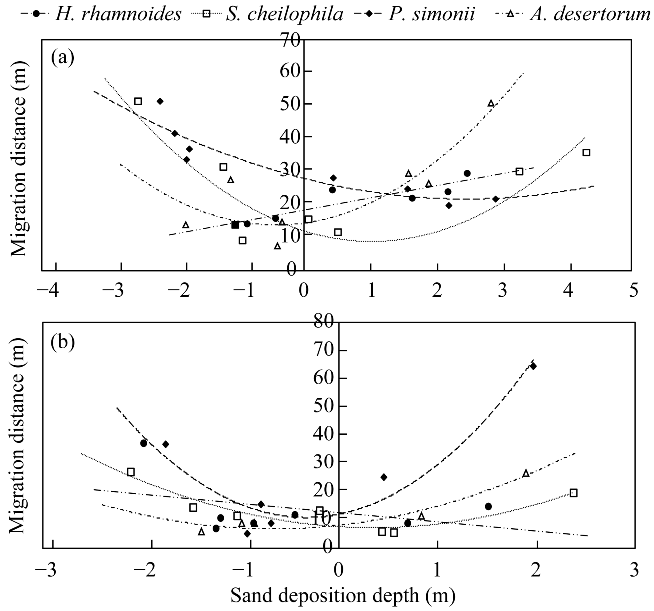

Fig. 7 Best fitting curves of sand deposition depth and migration distance of southward (a) and eastward (b) directions

4 Discussion

4.1 Factors of revegetated dune reforming

Micro-topography and plant structures influenced dunes aeolian differences basically through changing understory airflow field, and wind tunnel experiment tried to demonstrate and simulate aerodynamic and morphological process (Hesp et al., 2019; Walker et al., 2022). The original area, volume, and intervals of dunes restrained their expansion speed, direction, and spatial location to a certain degree (Lancaster, 1988; Li et al., 2021). A previous study of morphology of crescent

Table 2 Linear and quadratic fitting equations and significance test

Sample dune	Moving direction	Linear fitting equation	R^2	*t*-test	*P*	Quadratic fitting equation	R^2	*t*-test	*P*
Hr	Southward	$y=3.63x+18.28$	0.816	4.716	0.005	$y=-0.60x^2+4.49x+19.12$	0.831	2.647	0.057
	Westward	$y=-3.29x+12.39$	0.146	0.858	0.397	$y=6.65x^2-1.07x+3.42$	0.838	5.622	0.039
Sc	Southward	$y=-2.73x+30.77$	0.508	–0.605	0.567	$y=3.24x^2+2.72x+14.44$	0.790	–3.925	0.011
	Westward	$y=-1.48x+13.63$	0.088	0.481	0.519	$y=2.99x^2-2.10x+7.54$	0.870	13.357	0.017
Ps	Southward	$y=-4.60x+31.92$	0.807	–5.001	0.002	$y=1.01x^2-5.01x+27.93$	0.851	–5.294	0.003
	Westward	$y=11.15x+29.10$	0.434	3.072	0.155	$y=10.57x^2+6.96x+11.86$	0.920	17.316	0.023
Ad	Southward	$y=6.25x+21.92$	0.578	2.615	0.047	$y=2.97x^2-6.17x+12.12$	0.793	1.087	0.038
	Westward	$y=5.28x+12.70$	0.813	13.051	0.036	$y=2.87x^2+3.84x+8.00$	0.939	15.467	0.031

dunes and linear dunes revealed less shifting and migration at larger dune scales and higher knaps, which corresponds to slower migration and expansion observed in high-steep scale sample dunes (Joanna and Andreas, 2008; Bishop, 2010). *H. rhamnoides* and *P. simonii* dunes with medium scales expanded to south, but generally maintained their dome shape. *S. cheilophila* and *A. desertorum* dunes with low-flat scales variably changed from barchan to either dome or ribbon shaped dune to their small original volume and heavy sand accumulation around outline edges. A wide dune interval facilitates migration and expansion along with dominant wind direction, whereas narrower and deeper intervals form wind erosion through that impel turbulent airflow, leading to steep slopes and deep interdunes (Meire et al., 2014). For example, *A. desertorum* dunes invaded the lower *S. cheilophila* dunes from northeast to southwest, and high-steep *P. simoni* dunes had a trend of covering the lower dunes owing to narrow dune spacing. Meanwhile, yet considerable east-west and north-south movement was observed for dunes with wide spacing.

Artificial vegetation community development of revegetated dunes greatly enhanced their surface anti-erosion ability through soil-reinforcement by roots and the wind-breaking effects of branches. Evolved from mostly bare mobile dunes to fixed or semi-fixed revegetated dunes, they gradually deformed elliptically and exhibited reduced migration speed, which was mainly due to increased vegetation community coverage and species diversity (Follett and Nepf, 2012; Zhang et al., 2017). In alpine sandy land, tall shrub-tree plantation dominated more community resources and suppressed regrowth of native species, their simple community structures were more easily disturbed by wind–sand hazards, they were faster to degrade, and the same was true for high-steep scale dunes (Wu et al., 2020). Additionally, plant spacing, clear height (below-branch height), canopy porosity, and plant survival rate influenced airflow field with the increase in velocity and effective protection distance (Okin, 2008; Leenders et al., 2011; Chen et al., 2012). Moreover, heightened wind–sand activity restrained natural revegetation, leading to lower species diversity. In contrast, *H. rhamnoides* and *A. desertorum* dunes experienced lower wind energy under plants, and developed stable community owing to their high planting density and large horizontal canopy. Majority of high-steep scale dunes were subjected to excessive wind erosion and sand burial owing to unstable vegetation communities (Wu et al., 2020; Che et al., 2022).

4.2 Morphology evolution

Compared with that of regional tall barchan dunes with no vegetation cover, shape of revegetated dunes evolved more slowly and migrated wobbly (Momiji et al., 2002). Zhang et al. (2018) and Hu et al. (2021) found that the morphology of high-steep mobile dunes changed quickly from barchan shape to a dome or linear shape for less than 5 a. We found that leading wind of west-northwest-north directions caused bare shifting dunes to climb eastward and southward forming higher sand hills with sharpened sand ridges. In contrast, morphology of revegetated dunes mildly transformed into spindle or dome shapes with a flat knap and 2–3 blurred ridges and then extended southward and northward to connect with other dune wings, forming barchan chains and longitudinal dunes. Revegetated dunes exhibited a pattern of "cut-top, extended-slope,

stabilization, and internal unbalance" with the last phase typically presenting as an "ecological break" involving blowouts and the formation of erosion troughs and nebkhas in high-steep scales. In some cases, "ecological break" may be attributed to a new sand source that disrupts dune morphology (Zhu, 1963; Silc et al., 2020; Yamasaki et al., 2021).

Arid revegetated dunes quickly migrated and readily shifted into parabolic and linear shapes under the influence of wind storm and extreme drought, and possibly dismembered into nebhaks dunes within 10 a (Nickling and Wolfe, 1994; Hasi et al., 2013). Majority of semi-arid flat revegetated dunes evolved into fixed or semi-fixed sandy land owing to ecological restoration function and stable community structure of artificially planted vegetation. Furthermore, dune outlines dispersed and connected to each other, propelling sand-fixing and plant-recovery effects (Li, 2003). Alpine *S. cheilophila* and *P. simonii* dunes evolved into semi-fixed dunes with fragmentation shapes, whereas *H. rhamnoides* and *A. desertorum* dunes tended to have dome or longitudinal shapes. However, all revegetated dunes showed little movement in east-west directions owing to alternating dominant wind directions of northeast and northwest, but they faced the potential danger of dune activation and fragmentation, and presented the threats of invading southern grassland and inter-dune lowland.

5 Conclusions

Revegetated dunes progressed steadily from barchan to dome or ridge shapes, with four vegetation types contributing to topography reforming by knap planation, wing amplification, and slope symmetrization. Southward migration of wings was observed, indicating the need for sand-control in these areas. *H. rhamnoides* was found to be adaptive to each dune type and position, mitigating wind erosion, and slowing migration. *S. cheilophila* and *P. simonii* are recommended for afforestation efforts in medium and high-steep dunes' north wing and knap positions. *A. desertorum* revegetated dunes require additional reinforcement to increase anti-erosion and sand-fixing functions.

Conflict of interest

The authors declare that they have no known competing financial interests or personal relationships that could have appeared to influence the work reported in this paper.

Acknowledgements

This study was funded by the Jiangxi Provincial Natural Science Foundation (20202BABL213028), the Open Project of the State Key Laboratory of Plateau Ecology and Agriculture, Qinghai University, China (2022-KF-07), and the Doctoral Scientific Research Foundation of East China University of Technology (2019052, 2019045).

Author contributions

Conceptualization: WU Wangyang, ZHANG Dengshan; Methodology: WU Wangyang, TIAN Lihui; Investigation: WU Wangyang, TIAN Lihui, GAO Bin, YANG Dehui; Formal analysis: WU Wangyang; Project administration: TIAN Lihui; Resources and supervision: ZHANG Dengshan; Writing - original draft preparation: WU Wangyang, SHEN Tingting; Writing - review and editing: WU Wangyang, SHEN Tingting, GAO Bin, YANG Dehui.

References

Anthonsen K L, Clemmensen L B, Jensen J H. 1996. Evolution of a dune from crescentic to parabolic form in response to short-term climatic changes: Råbjerg Mile, Skagen Odde, Denmark. Geomorphology, 17(1–3): 63–77.

Barchyn T E, Hugenholtz C H. 2012. Predicting vegetation-stabilized dune field morphology. Geophysical Research Letters, 39: L17403, doi: 10.1029/2012GL052905.

Bhadra B K, Rehpade S B, Meena H, et al. 2019. Analysis of parabolic dune morphometry and its migration in Thar desert area, India, using high-resolution satellite data and temporal DEM. Journal of the Indian Society of Remote Sensing, 47(12): 2097–2111.

Bishop M A. 2010. Nearest neighbor analysis of mega-barchanoid dunes, Ar Rub' al Khali sand sea: The application of geographical indices to the understanding of dune field self-organization, maturity and environmental change. Geomorphology, 120(3–4): 186–194.

Bubenzer O, Bolten A. 2008. The use of new elevation data (SRTM/ASTER) for the detection and morphometric quantification of *Pleistocene megadunes* (draa) in the eastern Sahara and the southern Namib. Geomorphology, 102(2): 221–231.

Cao X, Jiao J Y, Liu J J, et al. 2022. Morphometric characteristics and sand intercepting capacity of dominant perennial plants in the Eastern Qaidam Basin: Implication for aeolian erosion control. CATENA, 210: 105939, doi: 10.1016/j.catena.2021.105939.

Chang X X, Chen H S, Li Z G, et al. 2021. Species diversity of ecological restoration plant communities in typical desert areas of the Brahmaputra River Basin in Tibet. Journal of Desert Research, 41(6): 187–194. (in Chinese)

Che C W, Xiao S C, Ding A J, et al. 2022. Growth response of plantations *Hippophae rhamnoides* Linn. on different slope aspects and natural *Caragana opulens* Kom. to climate and implications for plantations management. Ecological Indicators, 138: 108833, doi: 10.1016/j.ecolind.2022.108833.

Chen Z B, Ortiz A, Zong L J, et al. 2012. The wake structure behind a porous obstruction and its implications for deposition near a finite patch of emergent vegetation. Water Resources Research, 48(9): W09517, doi: 10. 1029/2012wr012224.

Durán O, Herrmann H J. 2006. Vegetation against dune mobility. Physical Review Letters, 97(18): 188001, doi: 10.1103/PhysRevLett.97.188001.

Follett E M, Nepf H M. 2012. Sediment patterns near a model patch of reedy emergent vegetation. Geomorphology, 179: 141–151.

Gillies J A, Nield J M, Nickling W G. 2014. Wind speed and sediment transport recovery in the lee of a vegetated and denuded nebkha within a nebkha dune field. Aeolian Research, 12(12): 135–141.

Hasi E, Du H S, Sun Y. 2013. *Caragana microphylla* nebkhas in Inner Mongolia plateau: Morphology and surface airflow. Quaternary Sciences, 33(2): 314–324.

Hesp P A, Dong Y, Cheng H, et al. 2019. Wind flow and sedimentation in artificial vegetation: Field and wind tunnel experiments. Geomorphology, 337: 165–182.

Hu G Y, Dong Z B, Zhang Z C, et al. 2021. Wind regime and aeolian landforms on the eastern shore of Qinghai Lake, northeastern Tibetan Plateau, China. Journal of Arid Environments, 188: 104451, doi: 10.1016/j.jaridenv.2021.104451.

Hugenholtz C H, Levin N, Barchyn T E, et al. 2012. Remote sensing and spatial analysis of aeolian sand dunes: A review and outlook. Earth-Science Review, 111(3–4): 319–334.

Joanna M, Andreas C W. 2008. The influence of different environmental and climatic conditions on vegetated aeolian dune landscape development and response. Global and Planetary Change, 64(1–2): 76–92.

Lancaster N. 1988. Controls of aeolian dune size and spacing. Geology, 16(11): 972–975.

Leenders J K, Sterk G, van Boxel J H. 2011. Modelling wind-blown sediment transport around single vegetation elements. Earth Surface Process Land, 36(9): 1218–1229.

Li J J, Jiao J Y, Cao X, et al. 2021. Spatial regionalization and response to morphological parameters of dune migration in the Qaidam Basin of China. Transactions of the Chinese Society of Agricultural Engineering, 37(7): 309–314.

Li Y F, Li Z W, Wang Z Y, et al. 2017. Impacts of artificially planted vegetation on the ecological restoration of movable sand dunes in the Mugetan Desert, northeastern Qinghai-Tibet Plateau. International Journal of Sediment Research, 32(2): 277–287.

Liu Z Y, Dong Z B, Cui X J. 2018. Morphometry of lunette dunes in the Tirari Desert. South Australia Open Geosciences, 10(1): 452–460.

Louis S. 2019. The fingerprint of linear dunes. Aeolian Research, 39: 1–12.

Meire D W S A, Kondziolka J M, Nepf H M. 2014. Interaction between neighboring vegetation patches: Impact on flow and deposition. Water Resource Research, 50(5): 3809–3825.

Miyasaka T, Okuro T, Miyamori E, et al. 2014. Effects of different restoration measures and sand dune topography on short- and long-term vegetation restoration in northeast China. Journal of Arid Environments, 111: 1–6.

Momiji H, Nishimori H, Bishop S R. 2002. On the shape and migration speed of a proto-dune. Earth Surface Processes and Landforms, 27(12): 1335–1338.

Nickling W G, Wolfe S A. 1994. The morphology and origin of nabkhas, region of Mopti, Mali, West Africa. Journal of Arid Environments, 28(1): 13–30.

Okin G S. 2008. A new model of wind erosion in the presence of vegetation. Journal of Geophysical Research Earth Surface, 113(2): F02S10, doi: 10.1029/2007JG000563.

Pang Y J, Wu B, Li Y H, et al. 2020. Morphological characteristics and dynamic changes of seif dunes in the eastern margin of

the Kumtagh Desert, China. Sciences in Cold and Arid Region, 12(5): 887–902.

Pike R J, Evans I S, Hengl T. 2009. Geomorphometry: A brief guide. Developments in Soil Science, 33: 3–30.

Qian G Q, Yang Z L, Luo W Y, et al. 2019. Morphological and sedimentary characteristics of dome dunes in the northeastern Qaidam Basin, China. Geomorphology, 350(1): 106923, doi: 10.1016/j.geomorph.2019.106923.

Rominger K, Meyer S E. 2019. Application of UAV-based methodology for census of an endangered plant species in a fragile habitat. Remote Sensing, 11(6): 719, doi: 10.3390/rs11060719.

Rozier O, Narteau C, Gadal C, et al. 2019. Elongation and stability of a linear dune. Geophysical Research, 46(24): 14521–14530.

Samuel A, Will F, Paul H. 2022. Quantifying vegetation and its effect on aeolian sediment transport: A UAS investigation on longitudinal dunes. Aeolian Research, 54: 100768, doi: 10.1016/j.aeolia.2021.100768.

Silc U, Steevi D, Lukovi M, et al. 2020. Changes of a sand dune system and vegetation between 1950 and 2015 on Velika Plaža (Montenegro, E Mediterranean). Regional Studies in Marine Science, 35: 101–139.

Walker I, Hesp P, Smyth T. 2022. Airflow dynamics over unvegetated and vegetated dunes. Treatise on Geomorphology, 7(2): 415–453.

Wang L X. 2000. Some opinions on the project or combating desertification in China. World Forestry Research, 13(6): 32–37. (in Chinese)

Wang T, Zhao H L. 2005. Fifty-year history of China desert science. Journal of Desert Research, 25(2): 145–165. (in Chinese)

Wu W Y, Zhang D S, Tian L H, et al. 2019. Features of artificial plant communities from the east sand region of the Qinghai Lake over the last 10 years. Acta Ecological Sinica, 39(6): 2109–2121. (in Chinese)

Wu W Y, Zhang D S, Tian L H, et al. 2020. Aeolian activities and protective effects of artificial plants in re-vegetated sandy land of Qinghai lake, China. Chinese Geographical Science, 30(6): 1129–1142.

Xiao J H, Xie X S, Zhao H, et al. 2021. Seasonal changes and migration of longitudinal dunes in the northeastern Rub'al Khali Desert. Aeolian Research, 51: 100710, doi: 10.1016/j.aeolia.2021.100710.

Xu Z, Mason J A, Lu H. 2015. Vegetated dune morphodynamics during recent stabilization of the Mu Us dune field, north-central China. Geomorphology, 228(1): 486–503.

Yamasaki T N, Jiang B, Janzen J G, et al. 2021. Feedback between vegetation, flow, and deposition: A study of artificial vegetation patch development. Journal of Hydrology, 598(8): 126232, doi: 10.1016/j.jhydrol.2021.126232.

Zhang D S, Zhang P, Wu W Y, et al. 2016. Wind-blown sand activity and control way of sand hazards at Ketu sandy land in eastern shore of the Qinghai Lake. Journal of Desert Research, 36(2): 274–280. (in Chinese)

Zhang M Y, Zhang D S, Wu W Y, et al. 2018. Application of UAV image based 3D reconstruction in morphological monitoring of dunes. Arid Land Geography, 41(6): 1341–1350. (in Chinese)

Zhang P, Kang J L, Yuan Z, et al. 2017. Similarities and differences of the plant communities on two vegetation-dunes and their responses to dune morphology. Acta Ecologica Sinica, 37(23): 7920–7927. (in Chinese)

Zheng Y, Yang Q, Ren H, et al. 2022. Spatial pattern variation of artificial sand-binding vegetation based on UAV imagery and its influencing factors in an oasis–desert transitional zone. Ecological Indicators, 141: 109068, doi: 10.1016/j.ecolind.2022.109068.

Zhu Z. 1963. Preliminary research on some problems of the dynamic processes of aeolian dune evolution. Geography Symposium, 5(1): 58–78. (in Chinese)